

Optical switching of one-dimensional photonic band gaps and coherent generation of dark and bright optical lattices in quantum wells

S. M. Sadeghi,^{1,*} W. Li,² X. Li,¹ and W.-P. Huang¹

¹*Department of Electrical and Computer Engineering, McMaster University, Hamilton, Ontario L8S 4K1, Canada*

²*Department of Chemical and Engineering Physics, University of Wisconsin-Platteville, Platteville, Wisconsin 53818, USA*

(Received 11 August 2005; published 4 January 2006)

We propose one-dimensional bright and dark optical lattices where Bragg scattering occurs, respectively, via periodic generation of gain without inversion and electromagnetically induced absorption in the absence of any refractive index perturbation. The absorption and gain processes are caused by quantum interference in the conduction intersubband transitions of a corrugated n -doped quantum well structure interacting with an intense infrared laser. The quantum well structure is embedded between two optical confinement layers, forming a periodic structure with a Bragg wavelength similar to that of the intersubband transition between the second and third conduction subbands of the quantum well. We show that in the absence of the intense infrared laser this transition is transparent, and the periodic structure forms a passive one-dimensional photonic gap generated by the background refractive index contrast of the corrugated region. In the presence of this laser, the intersubband transition is influenced by the quantum coherence effects, causing dramatic changes in the photonic band gap. We show that when one adjusts the intensity and wavelength of such a laser properly these effects can (i) destroy the one-dimensional photonic band gap, and (ii) form periodic regions of gain without inversion or electromagnetically induced loss, while the index perturbation is completely canceled out. Such bright and dark optical lattices can scatter a light at Bragg wavelength when its frequency is the same or close to that of the intersubband transition.

DOI: [10.1103/PhysRevB.73.035304](https://doi.org/10.1103/PhysRevB.73.035304)

PACS number(s): 73.21.Fg, 42.70.Qs, 42.65.-k, 42.70.Nq

I. INTRODUCTION

Dielectric periodic structures made from alternating non-resonant semiconductor materials have been extensively used for various applications. Prominent examples are distributed feedback (DFB) lasers,¹ optical filters,² optical switches,³ and others. These devices are based on the fact that when the period of the refractive index modulation in such structures is adjusted properly Bragg scattering occurs, causing a forbidden gap in transmission. Recently, however, utilization of such optical resonances along with the resonant electronic or excitonic transitions has promised a dramatic control over light propagation through periodic structures. In such structures, in contrast to the conventional photonic band gap (PBG) crystals, the signal field is resonant or near resonant with the electronic or excitonic transitions of the constituting semiconductor materials. Example of this includes a polaritonic active photonic band gap structure where the superradiant property of the optically coupled excitons in a multiquantum well structure is used to form a forbidden gap.⁴ It also includes application of quantum coherence in the intersubband transitions of n -doped quantum wells to generate an active one-dimensional (1D) photonic band gap using an infrared laser.⁵ An electromagnetically induced PBG associated with the atomic transitions has also been proposed in a heterostructure formed by semiconductor layers doped periodically with different densities of atoms. Here, the coherent nonlinear effects in these transitions create a periodic refractive index contrast.^{6,7}

Our objectives in this paper are to show how one can use an infrared (IR) laser beam (control field) near resonant with the intersubband transitions of an n -doped quantum well

(QW) structure to (i) destroy (switch off) a conventional 1D PBG by making the susceptibility of a periodic structure complex while diminishing its refractive index perturbation, and (ii) coherently induce periodic resonant or near-resonant gain and absorbing regions in the absence of any refractive index modulation, generating QW bright and dark optical lattices, respectively. The main idea behind these processes is the utilization of optical coherent effects caused by the control field in a corrugated structure made of several periods of the n -doped QW structure [Fig. 1(a)]. These effects include gain without inversion (GWI) and electromagnetically in-

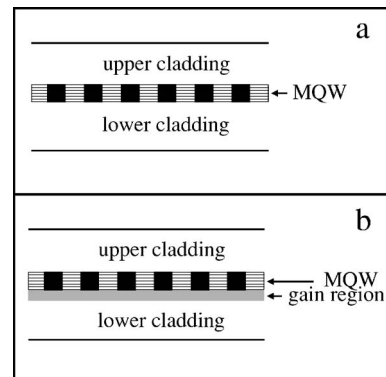


FIG. 1. Schematic representation of the waveguide structures used to study quantum well dark and bright optical lattices. The corrugated multiquantum well structure is located between the upper and lower cladding layers. The square black regions (trenches) refer to the quantum well regions that are etched and refilled epitaxially with a semiconductor material. The thick continuous gray line in (b) refers to the uniform gain layer.

duced absorption (EIA) accompanied by the coherent enhancement of refractive index in the conduction intersubband transitions of this structure. Here GWI refers to the gain that occurs when the population of the lower transition level is the same or more than the upper one. EIA, on the other hand, represents an absorption process between these two levels while their populations are inverted. Both GWI and EIA are associated with resonant enhancement of refractive index with zero absorption in the conduction intersubband transitions, similar to that in atomic systems,^{8–10} and are the results of quantum coherence in these transitions.

We show that in the absence of the control field the structure shown in Fig. 1(a) behaves as a conventional 1D PBG generated by the off-resonant (background) refractive index contrast of its constituting materials. However, as the intensity of this field increases, the signal field passing through this structure starts to feel a resonance. The resonant elements here are the periodic QW structure and the role of dipole active resonant excitations is played by the intersubband transitions. As this happens, the refractive index contrast of the corrugated QW structure and its surrounding in the waveguide structure shown in Fig. 1(a) diminishes, while the intersubband transitions become absorptive or develop gain. These processes alter light scattering along the waveguide and remove (switch off) the frequency band gap. With the total removal of the index perturbation, the waveguide structure has either a pure loss (dark optical lattice) or gain (bright optical lattice) corrugation. We show that when the signal field is resonant or near resonant with the conduction intersubband transitions and satisfies the Bragg condition, it can be coherently scattered by such optical lattices. This process, which occurs at the Bragg wavelength, allows one to use these lattices for various optical devices. These include laser sources that are intrinsically single-mode and very stable,¹¹ optical filters, time delay lines, and others.

Note that different schemes for generation of GWI in the intersubband transitions of quantum wells have been previously reported. These include utilization of coherent resonant tunneling,^{12–15} nonlinear wavemixing and frequency-down conversion,¹⁶ and a dc-coupling mechanism.¹⁷ EIA has also been studied in atoms by considering the interaction of a driving field with a degenerate two-level system.¹⁸ In addition, optical switching of polaritonic PBGs has been reported using ac Stark effect in the exciton lines or high photoexcited carrier densities to suppress super-radiant properties of excitons.¹⁹ In this paper, however, we are dealing with a switching process that leads to the full removal of the band gap by inducing quantum coherence in the conduction intersubband transitions. In addition, the dark and optical lattices introduced in this paper are different from those discussed in atomic systems. In such systems optical standing waves are responsible for trapping neutral atoms in spatial periodic potentials.²⁰ When the interaction of the atoms with the trapping beams is strong, these lattices are bright via Rayleigh scattering into their fluorescence spectra. On the other hand, when fluorescence of the trapped atoms is suppressed, they form dark optical lattices.²¹

II. ELECTRONIC CONDUCTION INTERSUBBAND TRANSITIONS IN THE PRESENCE OF OPTICAL RESONANCES

To study QW dark and bright optical lattices and optical switching of a conventional 1D PBG, we utilize resonant QW optical coherent processes combined with the photonic resonance associated with the waveguide structure shown in Fig. 1(a). In this structure a corrugated multi-QW structure is embedded between two optical confinement cladding layers. An IR laser (control field) with polarization along the growth direction (z) interacts with the QW structure, generating a strongly frequency-dependent complex susceptibility associated with the conduction intersubband transitions. Generally, light propagation in such a system can be treated using the following equation:

$$\left[\nabla_{y,z}^2 + \left(\frac{\omega_s}{c} \right)^2 \varepsilon^{\omega_c I_c}(\omega_s, y, z) \right] E^{\omega_c I_c}(\omega_s, y, z) = 0. \quad (1)$$

Here $\varepsilon^{\omega_c I_c}(\omega_s, y, z)$ refers to the dielectric permittivity of the structure for a given control field intensity (I_c) and frequency (ω_c). When this field is off ($I_c=0$) it has the following form:

$$\varepsilon^{\omega_c 0}(\omega_s, y, z) = \varepsilon_0(z) + \Delta\varepsilon^{\text{back}}(y, z). \quad (2)$$

Here ε_0 is related to the effective refractive index of the waveguide structure in the absence of the corrugated QW structure. $\Delta\varepsilon^{\text{back}}(y, z)$ is associated with the refractive index perturbation caused by the difference between the background indices of the QW regions and trenches along the propagation direction (y). Along the growth direction (z), this term is related to the refractive indices of the multilayer waveguide structure. Note that, as the right-hand side of Eq. (2) shows, the dielectric permittivity here does not depend on the signal field frequency (ω_s) and is responsible for formation of the off-resonant conventional 1D PBG. In the presence of the control field ($I_c \neq 0$), however, it becomes strongly frequency dependent

$$\varepsilon^{\omega_c I_c}(\omega_s, y, z) = \varepsilon_0(z) + \Delta\varepsilon_{\omega_c I_c}^{\text{res}}(\omega_s, y, z). \quad (3)$$

Here $\Delta\varepsilon_{\omega_c I_c}^{\text{res}}(\omega_s, y, z)$ represents variation of the dielectric function caused by the interaction of the control field with the corrugated QW structure used in the waveguide shown in Fig. 1(a). In fact, this term is associated with coherent enhancement of refractive index and generation of EIA and GWI in the conduction intersubband transitions of the QW.

To study how the evolution of $\varepsilon^{\omega_c I_c}(\omega_s, y, z)$ with the control field influences the conventional 1D PBG, we consider the n -doped QW used in Fig. 1(a) is a double structure as that shown in Fig. 2. This structure contains two $\text{In}_{0.5}\text{Ga}_{0.5}\text{As}$ wells separated by a 1.5 nm $\text{Al}_{0.5}\text{Ga}_{0.5}\text{As}$ barrier. The left and right barriers are, respectively, $\text{Al}_{0.4}\text{Ga}_{0.6}\text{As}$ and $\text{Al}_{0.55}\text{Ga}_{0.45}\text{As}$. As shown in Ref. 5, to generate these coherent effects one must use the control field to mix the first ($|1\rangle$) and third ($|2\rangle$) conduction subbands while the middle subband ($|1\rangle$) is not affected. Electrons from $|2\rangle$ decay into $|a\rangle$ and $|1\rangle$ via emission of longitudinal optical (LO) phonons. In addition, electrons in $|1\rangle$ can decay nonradiatively into $|a\rangle$ via tunneling. The signal field that experiences the periodic

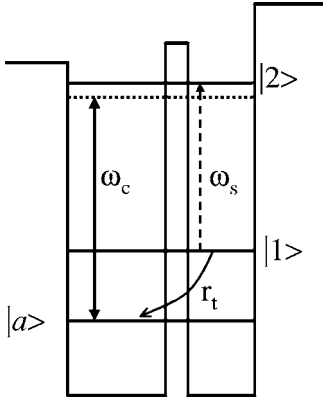


FIG. 2. Schematic diagram of the n -doped InGaAs/AlGaAs double QW structure. $|a\rangle$ is the ground state of the QW, and $|1\rangle$ and $|2\rangle$ are the lower and upper transition subbands, respectively. The two-sided arrow refers to the control field and the dashed one to the signal field. The curved arrow represents the tunneling process from $|1\rangle$ to $|a\rangle$.

complex susceptibility is in fact near resonant with the 1-2 transitions of such a QW. In the absence of the control field, as shown in the following, this field does not feel this transition as it is fully transparent under this condition and its refractive index (n) is the same as that of the background of the QW structure (n_b). Fig. 1(b) is similar to Fig. 1(a), except that here we consider a uniform semiconductor layer below the corrugated QW structure. This layer can be electrically or optically pumped, generating a uniform gain along the waveguide. The application of such a gain region will be discussed in the following section.

To study light scattering in the waveguide structures shown in Fig. 1 we first need to solve optical Bloch equations for the double QW structure. These equations can be obtained from the following

$$\frac{\partial \rho^{\mathbf{k}}}{\partial t} = -\frac{i}{\hbar} [H + H_{\text{int}}, \rho^{\mathbf{k}}] + \left. \frac{\partial \rho^{\mathbf{k}}}{\partial t} \right|_{\text{incoh}}^{e-e} + \left. \frac{\partial \rho^{\mathbf{k}}}{\partial t} \right|_{\text{incoh}}^{e-p}. \quad (4)$$

Here

$$H = \sum_{\mathbf{k}, i=a,1,2} E(i, \mathbf{k}) c_{i, \mathbf{k}}^\dagger c_{i, \mathbf{k}} \quad (5)$$

and

$$H_{\text{int}} = \hbar \sum_{\mathbf{k}} \{ \Omega_{a2} c_{a, \mathbf{k}}^\dagger c_{2, \mathbf{k}} + \Omega_{12} c_{1, \mathbf{k}}^\dagger c_{2, \mathbf{k}} + \text{H.c.} \}. \quad (6)$$

$E(i, \mathbf{k})$ is the energy eigenvalue of the quantum well (QW) wave function associated with the i th conduction subband. The operator $c_{i, \mathbf{k}}^\dagger$ creates an electron with wave vector \mathbf{k} in such a subband, and $c_{i, \mathbf{k}}$ annihilates the same electron. H_{int} is the interaction term between the double QW structure and the control (E_c) and signal (E_s) fields. $\Omega_{a2} = -\mu_{a2} E_c / \hbar$ and $\Omega_{12} = -\mu_{12} E_s / \hbar$ are the Rabi frequencies associated with these fields, where $\mu_{a2} = \langle z \rangle_{a2} \times e$ and $\mu_{12} = \langle z \rangle_{12} \times e$ (e is the electron charge). The second and third term in the right-hand side of Eq. (4) refer to the incoherent contributions of the electron-electron and electron-phonon scattering processes,

respectively. These terms are explained in Sec. III.

Solving Eq. (4) under the steady state condition we found the complex susceptibility of the QW structure shown in Fig. 2. This allowed us to calculate Eqs. (2) and (3). Having these two terms we then used a set of frequency-dependent coupled-mode equations to calculate the responses of the waveguide structures shown in Fig. 1. These equations are as follows:

$$\begin{aligned} \frac{dS_{\omega_c, I_c}(\omega_s)}{dz} - \left[\frac{\Gamma \alpha_{\omega_c, I_c}^{\text{res}}(\omega_s) + g}{2} - j\delta(\omega_s) \right] S_{\omega_c, I_c}(\omega_s) \\ = -j\kappa_{\omega_c, I_c}(\omega_s) R_{\omega_c, I_c}(\omega_s) \end{aligned} \quad (7)$$

$$\begin{aligned} \frac{dR_{\omega_c, I_c}(\omega_s)}{dz} + \left[\frac{\Gamma \alpha_{\omega_c, I_c}^{\text{res}}(\omega_s) + g}{2} - j\delta(\omega_s) \right] R_{\omega_c, I_c}(\omega_s) \\ = j\kappa_{\omega_c, I_c}(\omega_s) S_{\omega_c, I_c}(\omega_s). \end{aligned} \quad (8)$$

Here $S_{\omega_c, I_c}(\omega_s)$ and $R_{\omega_c, I_c}(\omega_s)$ refer to the forward and backward traveling waves, respectively. $\delta(\omega_s)$ is the detuning factor defined by $(\omega_s/c)n_{\text{eff}} - \beta_0$, where β_0 is the Bragg propagation constant and n_{eff} represents the effective refractive index of the waveguide. $\alpha_{\omega_c, I_c}^{\text{res}}(\omega_s)$ refers to the loss (ELA) or gain (GWI) generated in the corrugated QW structure by the coherent processes. They are proportional to the absorption coefficient of the 1-2 transition in Fig. 2. g is the gain in the uniform layer in the structure shown Fig. 1(b). Γ is the optical confinement factor, which is also a function of I_c and ω_c .

$\kappa_{\omega_c, I_c}(\omega_s)$ in Eqs. (7) and (8) refer to the complex coupling coefficient of the corrugated structures shown in Fig. 1. This parameter, which allows us to quantitatively investigate light scattering in the waveguide structure, is given by

$$\kappa_{\omega_c, I_c}(\omega_s) = \frac{\omega_s^2}{2\beta c^2} \frac{\int |\Phi|^2 \Delta \hat{\epsilon}_{\omega_c, I_c}^{\text{res}}(\omega_s, z) dz}{\int |\Phi|^2 dz}. \quad (9)$$

Here $\Delta \hat{\epsilon}_{\omega_c, I_c}^{\text{res}}(\omega_s, z)$ refers to the Fourier transform of $\Delta \epsilon_{\omega_c, I_c}^{\text{res}}(\omega_s, y, z)$ with respect to y . When $I_c=0$ this term should be substituted with the Fourier transform of $\Delta \epsilon^{\text{back}}(y, z)$. $\beta = \omega_s / n_{\text{eff}} c$ where c refers to the speed of light. Φ represents the cross-sectional optical mode profile, which also depends on the control field intensity and wavelength. Dropping the indices I_c and ω_c for simplicity, the real (κ_i) and imaginary (κ_g) parts of Eq. (9) are related to each other by

$$\kappa = \kappa_i + j\kappa_g. \quad (10)$$

When the control field is off, $\kappa_i \neq 0$ and $\kappa_g = 0$, and the waveguide structure generates a conventional 1D PBG caused by the background refractive index contrast of the QW regions and trenches. On the other hand, when wavelength and intensity of this field are properly adjusted, the signal field feels the 1-2 transitions and the structure becomes a resonant

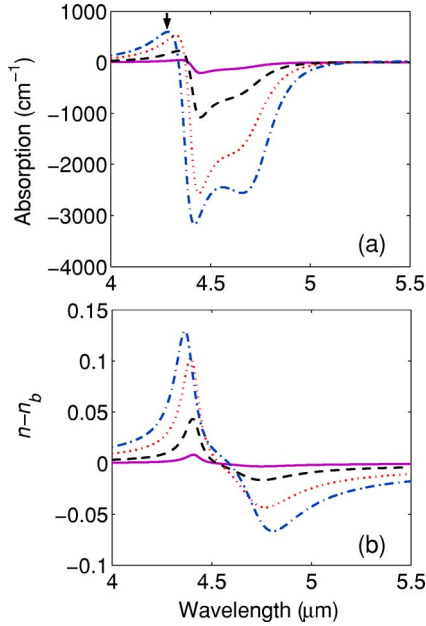


FIG. 3. (Color online) The absorption coefficient (a) and refractive index change (b) of the 1-2 transition. The solid, dashed, dotted, and dashed-dotted lines refer, respectively, to the simulation results obtained assuming $I_c=0.02, 0.12, 0.5,$ and 1.62 MW per cm^2 .

structure. Here, when $\kappa_g \neq 0$ and $\kappa_i=0$, we have either a dark or bright optical lattice.

III. OPTICAL SWITCHING OF PHOTONIC BAND GAP AND BRAGG DARK OPTICAL LATTICES CAUSED BY ELECTROMAGNETICALLY INDUCED ABSORPTION

To study optical switching of photonic band gaps and generation of a dark optical lattice via EIA we consider the thicknesses of the wide and narrow wells in the double QW structure shown in Fig. 2 are 4 and 2.5 nm, respectively. As a result, we find the energy spacing between $|a\rangle$ and $|1\rangle$ is 105 meV, nearly three times that of the LO phonon energy (34 meV). Therefore, we consider the tunneling rate of electrons from the 2.5 nm QW to 4 nm QW is 0.6 ps^{-1} .^{22,23} To further include the effects of electron-phonon scattering [third term in Eq. (2)], we consider the energy relaxation rates in the 1-2 and a -2 transitions caused by electron-LO-phonon scattering (Γ_{12}^{e-p} and Γ_{a2}^{e-p}) to be 2 and 3 ps, respectively.²⁴ The electron-electron scattering effects [second term of Eq. (4)] mostly affect the polarization decay rates associated with the 1- a and 2- a transitions (γ_{1a}^{e-e} and γ_{2a}^{e-e}). Here we consider these effects in a phenomenological way, considering the average rate of such a process in the ground subband (Γ_{aa}^{e-e}) is 4 ps^{-1} . Since in the presence of the control field the carrier densities in upper subbands still remain much smaller than that in the ground subband, we ignore this effect in these subbands. In addition, considering stain- and energy-dependent electron effective mass, the transition energies between $|1\rangle$ and $|2\rangle$ and between $|a\rangle$ and $|2\rangle$ were found 280 and 385 meV, respectively, with $\langle z \rangle_{12} = 2.2 \text{ nm}$ and $\langle z \rangle_{a2} = 0.7 \text{ nm}$.

Figure 3 shows absorption (a) and refractive index change (b) of the 1-2 transition for different values of the control field intensity (I_c) when the carrier density is assumed to be $6 \times 10^{11} \text{ cm}^{-2}$. We consider the wavelength of this field to be $3.36 \text{ } \mu\text{m}$, i.e., it is detuned from the a -2 transition by about 16.5 meV. When $I_c=0$ the 1-2 transition is transparent, with a refractive index the same as the background index of the QW structure ($n=n_b$). As shown in Fig. 3(a), as the intensity of this field increases, this transition starts to develop a large amount of gain. At the shorter wavelength side, however, the spectrum becomes absorptive (arrow). This occurs at a spectral range where the refractive index of the 1-2 transition is enhanced significantly [Fig. 3(b)]. Note that the absorption seen in Fig. 3(a) is an EIA process as it occurs with the presence of inversion. Such a process is the result of quantum coherence in the conduction intersubband transitions.

To see how these results can convert a 1D PBG into a dark optical lattice, we consider the corrugated QW system shown in Fig. 1(a) to consist of 80 periods of the QW structure depicted in Fig. 2. Although this structure is highly strained, it can be grown on a GaAs substrate using a graded $\text{In}_x\text{Al}_{1-x}\text{As}$ buffer layer. This layer allows accommodation of high strain and provides the optical confinement needed for the waveguide.²⁵ A possible growth recipe for this purpose involves deposition of $1 \text{ } \mu\text{m}$ or more of $\text{In}_x\text{Al}_{1-x}\text{As}$ over the GaAs substrate as x is linearly increased from 0 (AlAs) to 0.26 ($\text{In}_{0.26}\text{Al}_{0.74}\text{As}$). We assume that the QWs are etched and then refilled epitaxially with $\text{In}_x\text{Al}_{1-x}\text{As}$. Therefore, the fabrication techniques can be similar to those used for gain-coupled DFB lasers.^{26,27} Note that the In content (x) here is chosen such that, in the absence of the control field, the effective refractive indices of the trenches are higher than those of regions with QWs. We consider the corrugation period to be 673 nm , allowing the PBG and optical lattices to occur at the vicinity of $4.29 \text{ } \mu\text{m}$ in Fig. 3, where EIA accompanied with large refractive index enhancement occurs (arrow). The upper confinement layer is also taken to be $\text{In}_x\text{Al}_{1-x}\text{As}$ with an average refractive index of 3 at $4 \text{ } \mu\text{m}$ range, similar to that of the lower confinement layer.²⁸ At the same range the background refractive indices of the wells are considered 3.43, and those of the left and right barriers are 3.25 and 3.15, respectively. We consider the length of the waveguide to be $900 \text{ } \mu\text{m}$.

Having these in mind, Fig. 4(a) shows reflection of the waveguide structure shown in Fig. 1(a), when the control field is off ($I_c=0$). Under this condition we find $\kappa_i = 37.4 \text{ cm}^{-1}$ and $\kappa_g=0$, indicating a conventional 1D PBG caused by the contrast of background refractive indices of the corrugated structure. When the control field is turned on, the situation changes drastically. As shown in Fig. 4(b), for $I_c=0.12 \text{ MW per cm}^2$, the reflection diminishes to some extent while it is red shifted. This process corresponds to $\kappa_i = 31 \text{ cm}^{-1}$ and $\kappa_g=3 \text{ cm}^{-1}$. For $I_c=1.62 \text{ MW per cm}^2$, the situation changes more significantly as κ_i becomes nearly zero, i.e., refractive index perturbation along the waveguide structure vanishes, while $\kappa_g=11 \text{ cm}^{-1}$. Under these conditions the reflection develops a dim peak at the Bragg wavelength [Fig. 4(c)]. This indicates generation of a dark optical lattice where Bragg scattering is caused only by the pure loss

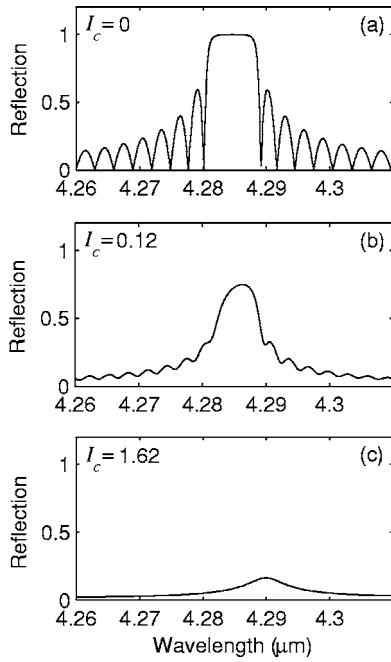


FIG. 4. Reflection of the waveguide structure shown in Fig. 1(a) for different control field intensities (I_c). (a) refers to the nonresonant that 1D PBG that occurred when $I_c=0$. (b) and (c) represent the cases where $I_c=0.12$ and 1.62 MW per cm^2 , respectively.

corrugation formed by EIA in the 1-2 transitions. In contrast to the case of Fig. 4(a), where the signal field did not feel the 1-2 transition, here it experiences a strong absorption associated with this transition. In fact, inspection of Figs. 3 and 4 shows that for the wavelength range influenced by the Bragg scattering such an absorption process does not strongly depend on the signal field frequency. At the same wavelength range, however, the refractive index of the 1-2 transition remains significantly dispersive. In general, to have dark or bright optical lattice, the absorption coefficient of this transition within this range should be either frequency independent or symmetric around the Bragg wavelength. This will be clarified further in the next section where within such a range both refractive index and gain are strongly frequency dependent.

Note that the drastic reduction of the reflection in Fig. 4(c) can be attributed mainly to the large amount of net loss caused by electromagnetically induced absorption (EIA) in the periodic QW regions. To study resonant Bragg scattering from the dark optical lattice caused by such a corrugation in more detail we need to compensate for this loss with some gain. As shown in Fig. 1(b), this can be done by adding a uniform gain layer to the waveguide structure in Fig. 1(a). As shown in Fig. 5, under the same conditions as those in Fig. 4(c) when the modal gain in this layer is considered to be 80 cm^{-1} , reflection of such a lattice can have a strong well-defined peak at the Bragg wavelength. Note that such a reflection is the result of the fact that the signal field is near-resonant with the 1-2 intersubband transitions and resonant with the photonic resonance associated with the periodic structure. Note also that the amplitude of the reflection in Fig. 5 depends on κ_g , the net loss of the waveguide, and the

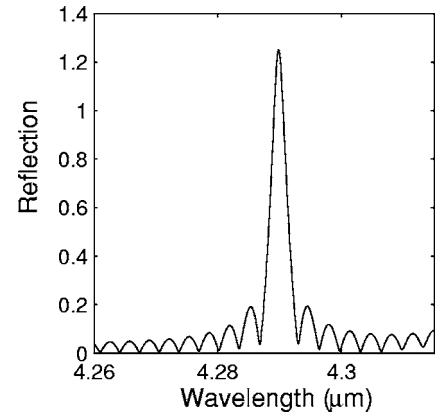


FIG. 5. Reflection of the dark optical lattice associated with the waveguide shown in Fig. 1(b) when the net loss is compensated by 80 cm^{-1} of uniform gain. All other specifications are the same as those in Fig. 4(c).

amount of the uniform gain. If one increases the amount of uniform gain to compensate for both mirror and internal losses, the waveguide structure acts as a purely loss-coupled DFB laser. Such a laser is intrinsically single mode at the Bragg wavelength.¹¹

The results presented in Fig. 4 showed that how one can coherently control light scattering in a waveguide structure using a laser field. Inspection of these results allows us to infer the mechanism behind optical switching of the 1D photonic band gap and formation of the dark optical lattice. To discuss this issue we show in Fig. 6 light dispersions associated with the results shown in Fig. 4. In this figure, $\delta/|\kappa|$ refers the normalized detuning of the signal field. Here $\delta = \beta - \beta_0$ where $\beta_0 = \bar{n}\omega_0/c$ refers to Bragg propagation constant and $\beta = \bar{n}\omega_s/c$ (\bar{n} is the average effective refractive index of the waveguide structure for given I_c and ω_c). $\text{Im}(\gamma)/|\kappa|$ refers to the normalized complex propagation constant where $\gamma^2 = \kappa^2 + (\alpha - i\delta)^2$.¹ Here α refers the average loss caused by EIA along the waveguide.

Figure 6(a) illustrates light dispersion associated with the passive 1D PBG in the absence of the control field [Fig. 4(a)]. It clearly shows that the width of the frequency band gap is proportional to κ_i , as one expects. As shown in Fig.

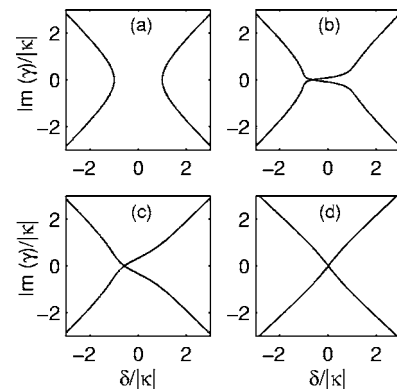


FIG. 6. Light dispersion associated with the results presented in Fig. 4. (a)–(d) correspond to $I_c=0$, 0.12 , 0.5 , and 1.62 MW per cm^2 , respectively.

6(b), the dispersion changes dramatically when the control field is turned on. Here light scattering is caused by the periodic variation of complex susceptibilities associated with the corrugated QW structure. Under such a situation if one adds some gain to the waveguide structure to overcome the total loss (mirror and internal losses), the structure acts as a loss-coupled DFB laser with a well-defined stop band and a dominant lasing mode.²⁹ As the intensity of the control field increases further, the refractive index contrast disappears, loss corrugation starts to become dominant, and ultimately a dark optical lattice is developed. Figures 6(c) and 6(d) show the overall evolutions of the light dispersion associated with these processes. Figure 6(d), in particular, shows the case when the QW dark optical lattice is fully developed, as the total absence of refractive index perturbation allows a symmetric dispersion around the Bragg wavelength ($\delta=0$).

IV. GAIN WITHOUT INVERSION AND QUANTUM WELL BRIGHT OPTICAL LATTICE

The results presented in the preceding section showed that when the intensity and frequency of the control field were adjusted properly the structure shown in Fig. 1(a) could set up periodic near-resonant absorbing regions in the absence of any spatial index perturbation. In this section, we study a QW bright optical lattice generated by spatial modulation of regions exhibiting resonant gain without inversion. For this we consider the same waveguide structure as that in the previous section [Fig. 1(a)], but decrease the number of the double QWs to 40. We also decrease the thickness of the narrow well to 2.2 nm. This increases the energy spacing between $|a\rangle$ and $|1\rangle$ to 131 meV and, therefore, compared to that in the preceding section, reduces the tunneling rate.^{22,23} We consider this rate to be 0.45 ps^{-1} . The slight modification of the double QW does not change the a -2 transition energy significantly but reduces that of 1-2 transition to 257 meV. The dipole moments of the a -2 and the 1-2 transitions were also obtained as $0.75e \times \text{nm}$ and $2.5e \times \text{nm}$, respectively. The carrier density in this structure is assumed to be $4 \times 10^{11} \text{ cm}^{-2}$.

Under these conditions, the absorption coefficient and refractive index change of the 1-2 transitions when the control field is resonant with the a -2 transition are shown in Fig. 7. Here, for any value of the control field intensity, the absorption spectrum contains a central gain region flanked between two absorption regions [Fig. 7(a)]. The gain here occurs in the absence of inversion (GWI) and is the result of quantum interference in the conduction intersubband transitions. Figure 7(b) shows the corresponding refractive index changes. Note that these results are similar to those seen in the atomic systems used to study resonant enhancement of refractive index with zero absorption.^{8,9} Here the enhancement process occurs at the crossing points of the gain and absorption regions where the absorption coefficient becomes zero, but the refractive indices of the intersubband transitions are increased.

Having these in mind, to study QW bright optical lattice we consider the length of the waveguide structure to be $350 \mu\text{m}$ and the period of the QW corrugation to be

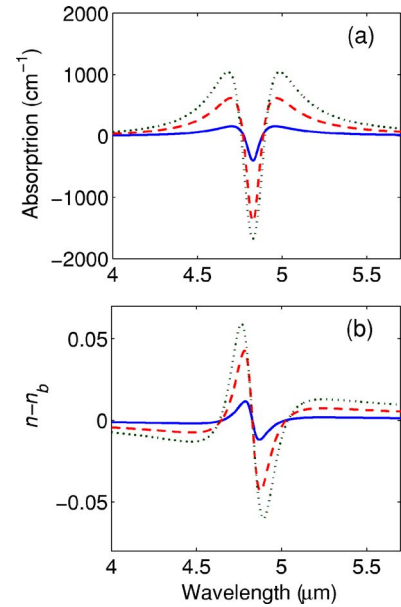


FIG. 7. (Color online) The absorption coefficient (a) and refractive index change (b) of the 1-2 transition when the control field is resonant with the a -2 transition in Fig. 2. The thin solid, dashed, and thick solid lines refer, respectively, to the simulation results obtained assuming $I_c=0.02, 0.11,$ and 0.42 MW per cm^2 .

783.5 nm. This allows us to have both intersubband and Bragg resonances at the same wavelength. In addition, we consider the In content (x) in the $\text{In}_x\text{Al}_{1-x}\text{As}$ filling layer such that, in the absence of the control field, the effective refractive indices of the trenches are slightly higher than

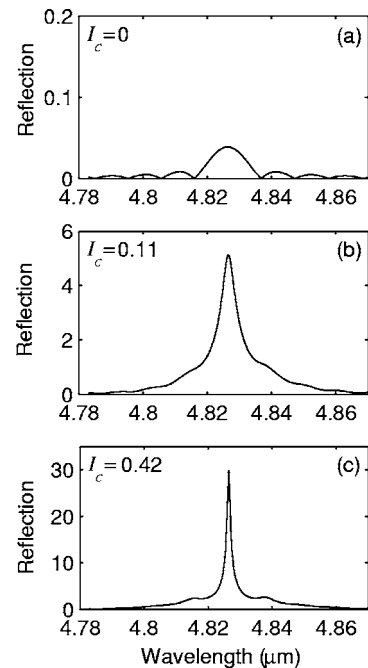


FIG. 8. Reflection of waveguide structure shown in Fig. 1(a) under the same conditions as those of Fig. 7 for various control field intensities (I_c). Here (a) refers to $I_c=0$, (b) to 0.11, (c) to 0.42 MW per cm^2 . All other specifications are the same as those in Fig. 7.

those of the regions with QWs. Under these conditions, variations of the waveguide reflection under different intensities of the control field are shown in Fig. 8. For $I_c=0$, due to the index corrugation, there is a slight amount of back reflection [Fig. 8(a)]. This is because of the fact that, compared to that in the preceding section, here the length of the wavelength is shorter and the refractive index contrast between QWs and trenches is much smaller. For $I_c=0.11$ MW per cm^2 , however, the residual of the index contrast is reduced significantly ($\kappa_i=-0.1 \text{ cm}^{-1}$) while κ_g becomes roughly 14 cm^{-1} [Fig. 8(b)]. This corresponds to the case where the back reflection mostly occurs due to the gain corrugation associated with the periodic regions with GWI. For $I_c=0.42$ MW per cm^2 , the contribution of κ_i remains insignificant while κ_g becomes 16.5 cm^{-1} [Fig. 8(c)]. The cases shown in Figs. 8(b) and 8(c) refer to the bright optical lattice limit where the waveguide structure has a nearly uniform effective refractive index, but light scattering occurs via periodic gain corrugation. Note that in these cases, the signal field is resonant with both the 1-2 transition and the photonic resonance associated with the Bragg scattering in the waveguide structure.

The results presented in Fig. 8 indicate that the bright optical lattice does not strongly depend on the control field intensity. In fact, with $I_c=0.11$ MW per cm^2 , we can see scattering at the Bragg wavelength. This situation does not change even when I_c becomes as large as 0.42 MW per cm^2 . The main effect of the field intensity here is to increase the gain corrugation contrast, as indicated by the increase of κ_g . This issue can be explained by considering the fact that within the wavelength range contributed to the light scattering and for the field intensities considered here, we have similar refractive index dispersions [dashed and dotted lines in Fig. 7(b)]. This happens for different amounts of gain at

the central wavelength. In any case, however, the bright optical lattices here are generated via strongly frequency-dependent refractive index and gain. In fact, within the wavelength range indicated in Fig. 8, the 1-2 transition has its maximum index and gain dispersions.

V. CONCLUSIONS

In conclusion, we studied the application of quantum coherence associated with the conduction intersubband transitions in n -doped quantum wells to generate dark and bright optical lattices and optically switch a 1D PBG. The optical lattices were composed of periodic arrangements of near-resonant absorbing and resonant gain regions in a waveguide structure in the absence of any refractive index variations. We showed that in the absence of the IR field responsible for the absorbing regions, the waveguide structure exhibited a nonresonant 1D PBG associated with the background refractive index contrast of the embedded corrugated QW structure. However, as the intensity of this field was increased, the structure developed a resonance. This allowed the corrugated QW structures in the waveguide to act as periodic resonant regions, forming dark optical lattice when they developed absorption via IR-induced coherent effects. We also showed that when the coherent effects generated gain without inversion in the periodic QW regions, a bright optical lattice was formed. In both of these cases, the refractive index contrast was totally canceled out via enhancement of refractive indices of the corrugated QW structure. We also showed that one could expect Bragg scattering of a signal field from these optical lattices, when its frequency satisfies the Bragg condition and/or being near-resonant or resonant with the conduction intersubband transitions.

*Electronic address: sadeghism@mail.ece.mcmaster.ca

¹H. Kogelnik and C. V. Shank, *J. Appl. Phys.* **43**, 2327 (1972).

²M. R. Fisher, S. Minin, and S. L. Chuang, *IEEE Photon. Technol. Lett.* **16**, 2084 (2004).

³K. Makatsuhara, T. Mizumoto, S. Hossain, S.-H. Joeng, Y. Tsukishima, B.-J. Ma, and Y. Nakano, *IEEE J. Sel. Top. Quantum Electron.* **6**, 143 (2000).

⁴M. Hubner, J. P. Prineas, C. Ell, P. Brick, E. S. Lee, G. Khitrova, H. M. Gibbs, and S. W. Koch, *Phys. Rev. Lett.* **83**, 2841 (1999).

⁵S. M. Sadeghi, W. Li, and H. M. van Driel, *Phys. Rev. B* **69**, 073304 (2004).

⁶Y. V. Rostovtsev, A. B. Matsko, and M. O. Scully, *Phys. Rev. A* **57**, 4919 (1998).

⁷Y. V. Rostovtsev, A. B. Matsko, and M. O. Scully, *Phys. Rev. A* **60**, 712 (1999).

⁸M. O. Scully and M. S. Zubiary, *Quantum Optics* (Cambridge University Press, Cambridge, England, 1997).

⁹U. Rathe, M. Fleischhauer, S. Y. Zhu, T. W. Hansch, and M. O. Scully, *Phys. Rev. A* **47**, 4994 (1993).

¹⁰A. S. Zibrov, M. D. Lukin, L. Hollberg, D. E. Nikonov, M. O. Scully, H. G. Robinson, and V. L. Velichansky, *Phys. Rev. Lett.*

76, 3935 (1996).

¹¹S. M. Sadeghi, W. Li, X. Li, and W.-P. Huang (unpublished) (2005).

¹²A. Imamoğlu and R. J. Ram, *Opt. Lett.* **19**, 1744 (1994).

¹³H. Schmidt and A. Imamoğlu, *Opt. Commun.* **131**, 333 (1996).

¹⁴H. Schmidt, D. E. Nikonov, K. L. Campman, K. D. Maranowski, A. C. Gossard, and A. Imamoğlu, *Laser Phys.* **9**, 797 (1999).

¹⁵D. E. Nikonov, A. Imamoğlu, and M. O. Scully, *Phys. Rev. B* **59**, 12212 (1999).

¹⁶A. A. Belyanin, F. Capasso, V. V. Kocharovskiy, V. V. Kocharovskiy, and M. O. Scully, *Phys. Rev. A* **63**, 053803 (2001).

¹⁷Y. Zhao, D. Huang, and C. Wu, *J. Opt. Soc. Am. B* **13**, 1614 (1996).

¹⁸A. Lezama, S. Barreiro, and A. M. Akulshin, *Phys. Rev. A* **59**, 4732 (1999).

¹⁹J. P. Prineas, J. Y. Zhou, and J. Kuhl, *Appl. Phys. Lett.* **81**, 4332 (2002).

²⁰G. Grynberg, B. Lounis, P. Verkerk, J. Y. Courtois, and C. Salomon, *Phys. Rev. Lett.* **70**, 2249 (1993).

²¹A. Hemmerich, M. Weidmuller, T. Esslinger, C. Zimmermann, and T. Hansch, *Phys. Rev. Lett.* **75**, 37 (1995).

- ²²S. Khan-ngern and I. A. Larkin, *Phys. Lett. A* **266**, 209 (2000).
- ²³O. Gauthier-Lafaye, P. Boucaud, F. H. Julien, S. Sauvage, S. Cabaret, and J.-M. Lourtioz, *Appl. Phys. Lett.* **71**, 3619 (1997).
- ²⁴J. Faist, F. Capasso, C. Sirtori, D. Sivco, J. Baillargeon, A. Hutchinson, S.-N. G. Chu, and A. Cho, *Appl. Phys. Lett.* **68**, 3680 (1996).
- ²⁵D. S. Katzer, W. S. Rabinovich, and G. Beadie, *J. Vac. Sci. Technol. B* **18**, 1614 (2000).
- ²⁶G. P. Li, T. Makino, R. Moore, N. Puetz, K. W. Leong, and H. Lu, *IEEE J. Quantum Electron.* **29**, 1736 (1993).
- ²⁷N. Nunoya, M. Nakamura, M. Morshed, S. Tamura, and S. Arai, *IEEE J. Sel. Top. Quantum Electron.* **7**, 249 (2001).
- ²⁸J. H. Beak, B. Lee, S. W. Choi, J. H. Lee, and E. Lee, *Appl. Phys. Lett.* **68**, 2355 (1996).
- ²⁹M. Funabashi, H. Kawanishi, T. K. Sudoh, T. Nakura, D. Schmitz, F. Schulte, Y. Nakano, and K. Tada, *International Conference on Indium Phosphide and Related Materials*, Cape Cod, MA, 1997, p. 292.